

Field emission from diamond-coated multiwalled carbon nanotube “teepee” structures

Y. Zou, P. W. May, S. M. C. Vieira, and N. A. Fox

Citation: *J. Appl. Phys.* **112**, 044903 (2012); doi: 10.1063/1.4748336

View online: <http://dx.doi.org/10.1063/1.4748336>

View Table of Contents: <http://jap.aip.org/resource/1/JAPIAU/v112/i4>

Published by the [American Institute of Physics](#).

Related Articles

Improving the field emission of carbon nanotubes by lanthanum-hexaboride nano-particles decoration
Appl. Phys. Lett. **101**, 123116 (2012)

Analysis of field-emission from a diamond-metal-vacuum triple junction
J. Appl. Phys. **112**, 066102 (2012)

Ultra-high current density carbon nanotube field emitter structure on three-dimensional micro-channeled copper
Appl. Phys. Lett. **101**, 063110 (2012)

Shot noise of low energy electron field emission due to Klein tunneling
J. Appl. Phys. **112**, 016104 (2012)

Direct observation and mechanism of increased emission sites in Fe-coated microcrystalline diamond films
J. Appl. Phys. **111**, 124309 (2012)

Additional information on J. Appl. Phys.

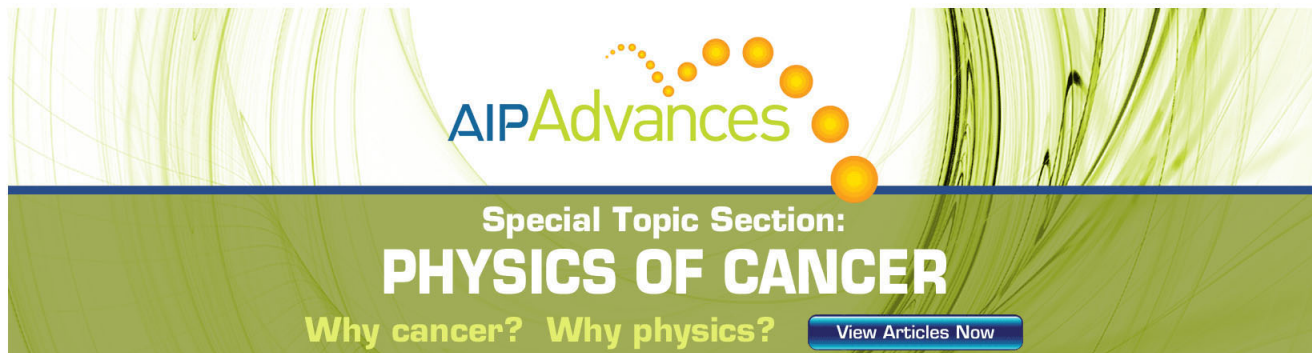
Journal Homepage: <http://jap.aip.org/>

Journal Information: http://jap.aip.org/about/about_the_journal

Top downloads: http://jap.aip.org/features/most_downloaded

Information for Authors: <http://jap.aip.org/authors>

ADVERTISEMENT



AIP Advances

Special Topic Section:
PHYSICS OF CANCER

Why cancer? Why physics? [View Articles Now](#)

Field emission from diamond-coated multiwalled carbon nanotube “teepee” structures

Y. Zou,^{1,a)} P. W. May,^{2,b)} S. M. C. Vieira,³ and N. A. Fox²

¹*School of Materials Science and Engineering, Nanjing University of Science and Technology, No. 200 Xiaolingwei, Nanjing 210094, Jiangsu Province, People's Republic of China*

²*School of Chemistry, University of Bristol, Bristol BS8 1TS, United Kingdom*

³*Instituto de Engenharia de Sistemas e Computadores - Microsistemas e Nanotecnologias (INESC MN/IN), Rue Alves Redol 9, 1000-029 Lisboa, Portugal*

(Received 16 April 2012; accepted 31 July 2012; published online 28 August 2012; corrected 31 August 2012)

Dense arrays of vertically aligned multiwalled carbon nanotubes (MWCNTs) have been seeded with a nanodiamond suspension in methanol using electrospray deposition. This treatment caused the tips of groups of 20–40 MWCNTs to stick together forming structures resembling “teepees.” Subsequent short chemical vapour deposition experiments using standard diamond-growing conditions allowed the nanodiamond seeds to grow into a thin continuous film, locking the teepee structures into this shape. Field emission tests show that these diamond-coated carbon nanotubes (CNTs) teepees retain the low threshold voltage of the uncoated CNTs but with greatly improved emission stability and lifetime. © 2012 American Institute of Physics. [<http://dx.doi.org/10.1063/1.4748336>]

I. INTRODUCTION

The use of carbon nanotubes (CNTs) as electron sources for field emission (FE) applications has generated wide interest since their identification in 1991. FE has been investigated from individual nanotubes^{1,2} and from CNT ensembles,^{3–5} with low threshold voltages and high efficiencies being generally observed,⁶ partly as a result of the high electrical conductivity of the nanotubes but also due to the extremely high geometrical field-enhancement effect at the nano-sharp tip.⁷ However, the poor lifetime and erratic stability of the emission current from these sources have been one of the chief obstacles preventing their commercial viability.⁸ When CNT field emitters operate under moderate vacuum conditions they suffer from long-term degradation due to the adsorption of gas molecules on their surface, resulting in tip “burn-out” and the emission ceasing.⁹ To overcome this shortcoming, other materials have been investigated as potential field emitters, including wide-band gap materials, such as diamond, aluminum nitride, boron nitride, and lithium fluoride.^{10–13} Of these, diamond films made by chemical vapour deposition (CVD) are perhaps the most promising, owing to their negative-electron-affinity (NEA) surfaces with low effective work functions.^{14–17} The FE properties of diamond can be enhanced by reducing the grain-size,¹⁸ doping it with boron to increase its conductivity,¹⁹ modifying the surface chemistry with different functional groups (such as CsO^{20,21} or LiO²²) to alter the NEA, and/or fabricating the diamond into sharp tips to increase the field enhancement factor.²³ However, despite these efforts, the relatively poor conductivity of CVD diamond, its columnar grain structure, the difficulty in making low-resistance back contacts, and processing difficulties, have meant that

diamond-based FE devices usually have higher threshold voltages and are less efficient when compared with the equivalent CNT-based FE devices.¹⁶ Nevertheless, diamond-based FE devices do not suffer tip burn-out to the same degree as CNT devices, and therefore have considerably longer lifetimes.

The purpose of the work reported here was to combine the excellent conductivity of CNTs with the robustness and long lifetime of a diamond surface, to create highly efficient, yet long-lived FE devices. There are several recent reports on development of such hybrid materials comprising diamond and CNTs.^{24–29} Although some success has been reported in increasing the time to burn-out by these methods, the FE characteristics were generally not greatly improved due to the fact that the CNTs were randomly oriented and often lying down on the substrate surface. Our approach is to put a thin CVD diamond coating onto vertically aligned CNTs, which requires three stages: (i) deposition of dense vertically aligned CNTs, (ii) seeding the CNT tips with nanodiamond particles to encourage diamond growth, and (iii) depositing CVD diamond sufficient to form a thin coating without completely embedding the CNTs within the diamond film.

II. EXPERIMENTAL

Preliminary experiments were performed upon single-walled CNTs. Unfortunately, standard CVD diamond conditions are designed to etch graphitic material back into the gas phase while simultaneously depositing diamond.³⁰ As a result, we found that singlewalled CNTs often completely etched away before a continuous diamond coating could form on the surface. Multiwalled carbon nanotubes (MWCNTs) are more robust, and although some etching will occur, they can withstand the CVD conditions long enough for a continuous diamond coating to form, at which point the graphitic CNT is shielded from the reactive etchant gas allowing the diamond growth to continue indefinitely.

^{a)}Author to whom correspondence should be addressed. Electronic mail: yshzou75@gmail.com.

^{b)}email: paul.may@bris.ac.uk.

The MWCNTs were grown in a dc plasma enhanced (PE) CVD reactor. After ultrasonically cleaning the single-crystal Si (100) substrate material using acetone and isopropanol, a 40 nm layer of SiO₂ followed by a 7 nm layer of Ni was sputtered onto the surface. The SiO₂ acted as a protective layer to prevent the Ni catalyst reacting with the Si to form Ni_xSi_y. These substrates were then placed inside the CVD reactor chamber and the temperature raised to 970 K in a gas mixture of C₂H₂/NH₃ (50 sccm/200 sccm) for 10 min. This caused the Ni coating to partially melt and form isolated Ni nano-particles positioned randomly across the surface, which acted as catalysts upon which the CNTs could nucleate. A dc bias was set at 650 V to ensure that the CNTs grew vertically aligned with respect to the substrate surface. The length, diameter, and density of the CNTs could be varied by changing the growth conditions; the variation in FE characteristics with these properties will be presented in a subsequent publication. For now, we shall focus on one representative set of vertically aligned CNTs of length $\sim 5 \mu\text{m}$, width 20–50 nm, and areal density $\sim 1 \times 10^9 \text{ cm}^{-2}$, as shown in Figure 1. The CNTs each have a small amount of residual catalyst embedded at the growth tip (Figure 1(c)).

In order to promote CVD diamond growth, the CNTs were seeded using a suspension of 5 nm-diameter detonation nanodiamond (DND) particles³¹ in a suspension of methanol. The DND particles had previously been acid cleaned and sonicated for an hour to break up any aggregates. The DND-methanol colloidal suspension was then sprayed onto the surface of the CNT array using a home-built electro spray system.³² The electrostatic spray (“electrospray”) deposition

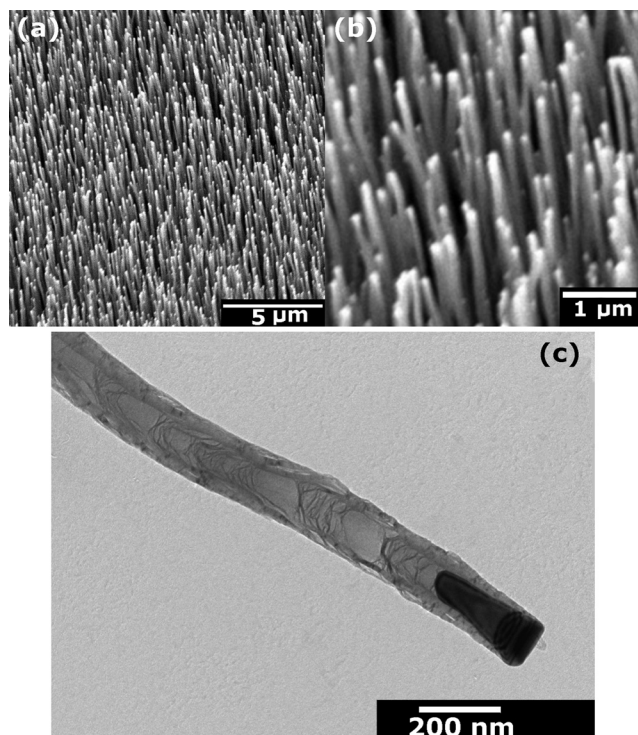


FIG. 1. SEM images of the vertically aligned MWCNTs at (a) low and (b) higher magnification. (c) A transmission electron microscope image showing the presence of the solid Ni catalyst particle remaining inside the tip of the CNTs.

technique uses a large potential difference to ionize nucleating particles (or droplets containing the particles) via the corona effect and accelerates them towards a grounded substrate.

Approximately, 1 ml of the colloidal suspension was placed in a plastic syringe located on the outside of an insulating box, as shown in Figure 2. The metal syringe needle passed through the wall of the box by turning through 90° and once inside the box bends upwards to point the nozzle toward the substrate. A 35 kV bias was applied to the metal tip of the nozzle which was sufficient to ionize the droplets without becoming unstable and arcing. The Si substrate containing the CNT array was positioned $\sim 50 \text{ mm}$ away from the nozzle on a rotating conducting mount. The mount was well grounded, ensuring that ionized aerosols emanating from the nozzle would be attracted along electric field lines towards the substrate. Rotating the substrates on the mount at up to 1500 rpm enabled uniform layers to be deposited onto substrates up to 4 cm in diameter. The potential difference pulls the suspension through the capillary, removing the need to apply a driving pressure, while charging prevents the droplets coalescing. Adjusting the nozzle-to-substrate distance is a crucial parameter, since this determines how much of the methanol evaporates from the droplets during flight. For coating CNT arrays, we found that $\sim 75\%$ evaporation was optimum. Less than this and too many CNTs would stick together forming flattened patches or “splashes”; more than this, and mostly dry DND particles would strike the CNTs leading to none of the CNTs sticking together.

III. RESULTS

Figure 3 shows scanning electron microscope (SEM) images of the CNT arrays following electro spray seeding. The remaining methanol in the droplets striking the top surface of the CNT array has wetted the CNTs, and electrostatic attraction has then clumped several tips together to meet at a point, forming a structure resembling a Native American “teepee.” The number of CNTs forming each teepee depends upon their areal density. This chosen set of CNTs with areal density $\sim 1 \times 10^9 \text{ cm}^{-2}$ results in 30–40 CNTs clumping together with a teepee density of $\sim 10^7 \text{ cm}^{-2}$. The teepees are stable in air for several weeks. The role, if any, played in this clumping process by the metallic catalyst embedded within each CNT tip is under investigation.

The seeded teepee structures were then placed into a hot-filament CVD reactor in order to grow a thin layer of

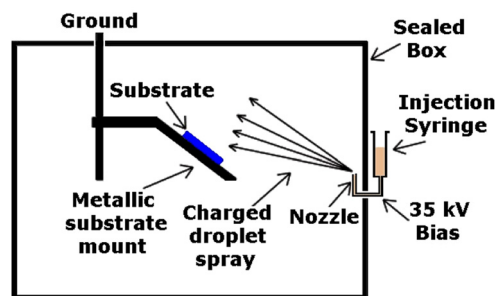


FIG. 2. Schematic diagram of the electro spray apparatus.³²

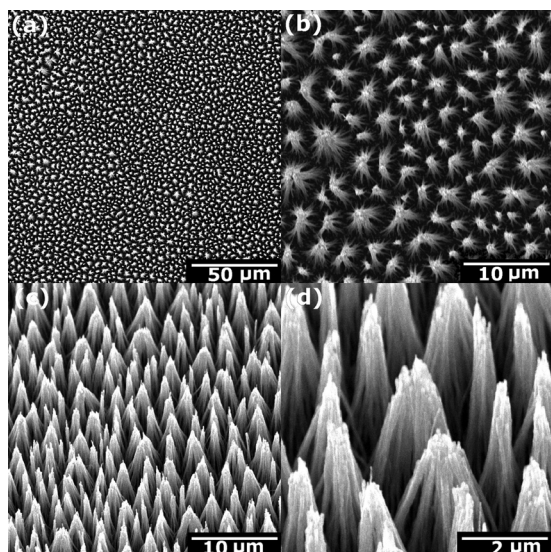


FIG. 3. SEM images of MWCNTs after electro spray seeding with a DND-methanol suspension. (a) and (b) top views, (c) and (d) images taken with sample tilted at 45° . The DND particles are present on the surface of the CNTs but are too small to be seen at these magnifications.

diamond over the surfaces of the CNTs. Standard diamond CVD conditions²⁸ were used: pressure 20 Torr, 1%CH₄/H₂ gas mixture, total flow 200 sccm, Ta filament placed 5 mm above the substrate surface, filament temperature 2400 K, substrate temperature ~ 1200 K. The growth times were kept short, between 30 min and 1 h, to ensure that only a thin film of diamond was formed as a protective layer on top of the teepees, as shown in Figures 4(a) and 4(b), and to avoid the teepees being completely embedded within a thicker film, as in Figure 4(c). Other samples were made using 5000 ppm B₂H₆ in the gas mixture to produce B-doped p-type diamond with near metallic conductivity, and with teepee morphology

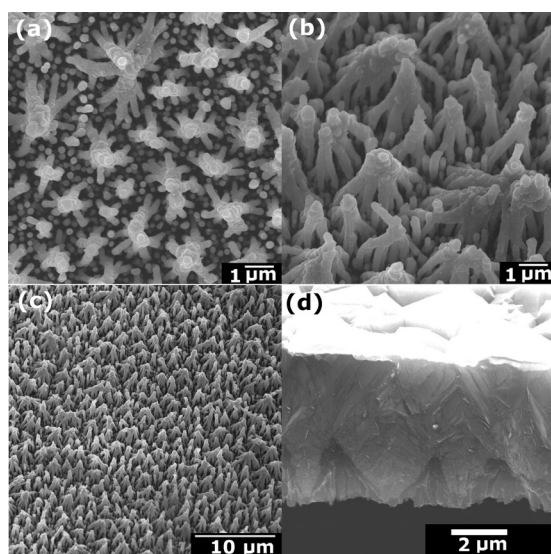


FIG. 4. SEM images of the teepee structures after 30 min diamond CVD. (a) Top view, (b) and (c) sample tilted at $\sim 45^\circ$. The teepee structures have been retained with the MWCNTs being conformally coated in a layer of undoped diamond. (d) Cross-sectional SEM image showing that after 8 h CVD, the teepees have been buried beneath the $5 \mu\text{m}$ -thick diamond film.

similar to those for the undoped films shown in Figures 4(a) and 4(b).

Laser Raman analysis (Figure 5) from the thinly coated undoped samples shown in Figures 4(a) and 4(b) is consistent with the coatings being nanocrystalline diamond.

FE measurements were performed on the original CNT arrays and the undoped and B-doped diamond-coated teepees using a parallel-plate configuration in a vacuum chamber at 5×10^{-7} Torr. The samples acted as the cathode, and a phosphor screen coated with a 10 nm layer of gold or aluminum acted as the anode, with a silica spacer maintaining a fixed separation of $d = 150 \mu\text{m}$ between the two plates. The emission current, I , was measured as the voltage on the anode, V , was increased. For the uncoated CNT samples, several “conditioning” runs were required before a stable I - V curve could be achieved, but for both the diamond-coated teepee samples, no conditioning was necessary – the I - V curves were reproducible from the first measurement. The phosphor screen emitted light when struck by the FE electrons, and this permitted the area over which the electron emission occurred, A , to be estimated. To normalize the data, therefore, we have plotted emission current density, J ($=I/A$ in A cm^{-2}) versus electric field, E ($=V/d$ in $\text{V } \mu\text{m}^{-1}$) and also as a Fowler-Nordheim plot¹⁵ ($\ln(J/E^2)$ versus $1/E$), as shown in Figure 6. For approximately the same measured current, we observed that the emission from the CNT arrays came from a much larger area than that from the teepees, and therefore the current density for the CNT arrays is much smaller.

As can be seen from Figure 6, the data are consistent with the Fowler-Nordheim model for electron emission via tunneling through a potential barrier for both the CNT and teepee samples.¹⁵ The threshold field corresponding to an electron emission density of 0.01 mA cm^{-2} from the uncoated CNTs was $\sim 3.13 \text{ V } \mu\text{m}^{-1}$, which is consistent with values reported in the literature for similar CNT systems.⁶

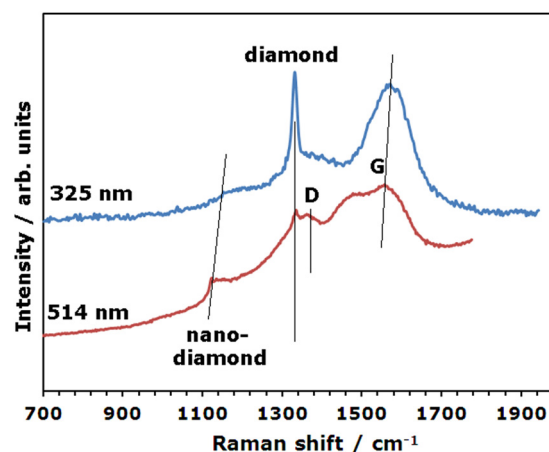


FIG. 5. Laser Raman spectra (514 nm and 325 nm excitation), from the diamond-coated CNT teepees shown in Figures 4(a) and 4(b), showing the sp^3 diamond peak at 1332 cm^{-1} , the D and G bands due to disordered sp^2 carbon at ~ 1350 and $1550\text{--}1600 \text{ cm}^{-1}$, respectively, and the “nanodiamond” peak at $\sim 1120\text{--}1180 \text{ cm}^{-1}$ due to sp^2 carbon at the grain boundaries of nanocrystals.³³ As expected, the diamond peak shows no dispersion (increase in peak wavenumber with excitation energy), whereas the G-band shows a only small dispersion. The nanodiamond peak shows a substantial dispersion consistent with the value of $\sim 31 \text{ cm}^{-1}/\text{eV}$ reported by Wagner and co-workers.³⁴

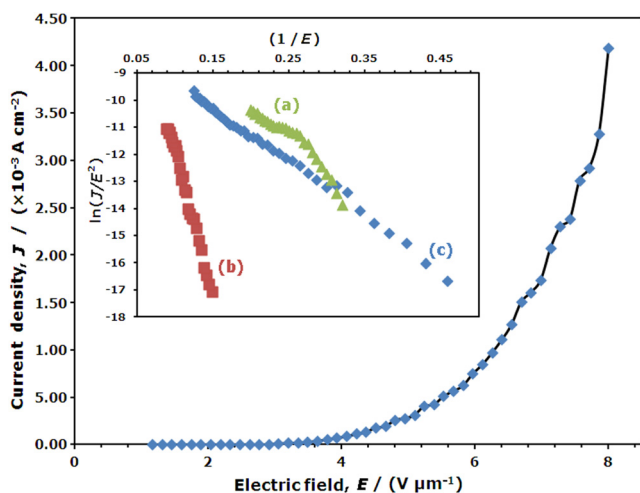


FIG. 6. FE characteristics of the CNT arrays and the diamond-coated CNT teepees. A typical curve of current density, J , versus electric field, E , for the B-doped-diamond-coated teepees (average of 5 data sets). Inset: Fowler-Nordheim plots from the 3 types of sample: (a) uncoated CNTs, (b) undoped-diamond-coated teepees, (c) B-doped-diamond-coated teepees.

For the undoped diamond-coated CNT teepees, the threshold field increased to $7.46 \text{ V } \mu\text{m}^{-1}$, presumably due to the insulating nature of the diamond coating through which the electrons have to travel to reach vacuum. Consistent with this model, for the conducting B-doped-diamond-coated teepees, the threshold field was $\sim 3.0 \text{ V } \mu\text{m}^{-1}$.

Stability tests were performed on the 3 types of sample by measuring the emission current as a function of time for a period of 2000 min (33 h). Again, due to the larger emission area for the uncoated CNTs, the emission density was lower for these than for the teepees. This means that the CNTs were not being driven as hard as the teepees, and might therefore be expected to have a longer lifetime. In fact, the opposite is true. As can be seen from Figure 7, the two teepee samples showed less variation with time (flicker) than the CNT sample, with no drop-off in intensity for the whole testing period. In contrast, the uncoated CNT sample showed considerable flicker, and the emission current gradually decreased with time due to progressive nanotube burn-out, with the test ending when the current density became too low at ~ 1000 min.

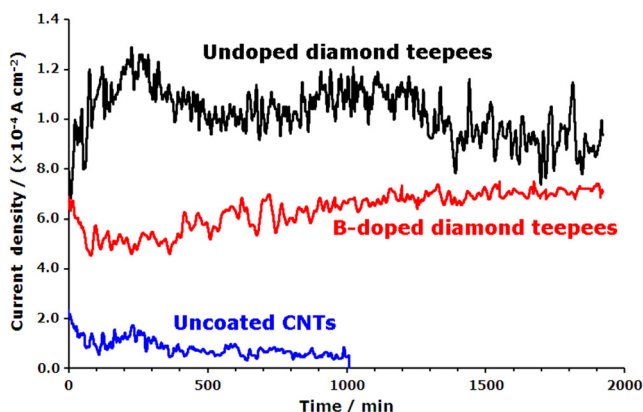


FIG. 7. FE current-density stability test from the uncoated CNTs, undoped diamond-coated teepees, and B-doped-diamond-coated teepees.

IV. CONCLUSIONS

In summary, we have described a novel method to fabricate diamond-coated CNTs resulting in teepee-shaped structures which are ideal for FE applications. Due to their density, morphology, and uniformity, such teepee structures may also be useful as electrochemical electrodes and in hydrogen storage applications. A conducting B-doped diamond coating on these teepees exhibits the same desirable low FE threshold voltage of uncoated CNTs, while significantly improving the lifetime, stability, and flicker characteristics. We propose that this may be due to the combination of the excellent electrical conductivity and transport properties of the CNTs, the good electrical contact between the CNT and the Si substrate, and the robust NEA surface of the diamond coating. The fact that 30–40 CNTs form each teepee structure may allow an increased current through the tip (compared to that from a single CNT), despite the field enhancement factor being smaller for the larger more-rounded teepee tip than for a single sharp CNT. Another factor may be the physical separation of the teepee structures (typically $1\text{--}2 \mu\text{m}$) which may help reduce space-charge effects that often limit emission current in densely packed devices.

There are still many parameters, such as the length, areal density, and thickness of the CNTs, the diamond growth morphology (microcrystalline, nanocrystalline), B-doping level, growth time, and other diamond surface terminations to vary the NEA properties (H, CsO, LiO, etc), which still need to be explored to optimize the FE characteristics, and these experiments are currently underway.

ACKNOWLEDGMENTS

We thank James Smith, Gareth Fuge, and Fernando Silva for technical assistance, and Mike Ashfold for useful input to this work. We also thank Bill Milne from the University of Cambridge, Department of Engineering for invaluable assistance with the CNT deposition during the early stages of the project. Part of this work was financed by the Portuguese Foundation of Science and Technology (FCT) with project Ref. No. PTDC/CTM/103121/2008. S. M. C. Vieira acknowledges FCT for financial support through the Ciência2007 program. Y. Zou thanks the China Scholarship Council, National Nature Science Foundation of China (51002078), QingLan Project of Jiangsu Province for financial support.

¹R. C. Smith, J. D. Carey, R. D. Forrest, and S. R. P. Silva, *J. Vac. Sci. Technol. B* **23**, 632 (2005).

²R. C. Smith, D. C. Cox, and S. R. P. Silva, *Appl. Phys. Lett.* **87**, 103112 (2005).

³W. A. de Heer, A. Chatelain, and D. Ugarte, *Science* **270**, 1179 (1995).

⁴Y. Saito, K. Hamaguchi, T. Nishino, K. Hata, and K. Tohji, *Jpn. J. Appl. Phys., Part 2* **36**, L1340 (1997).

⁵J.-M. Bonard, J.-P. Salvetat, T. Stöckli, L. Forró, and A. Châtelain, *Appl. Phys. A: Mater. Sci. Process.* **69**, 245 (1999).

⁶Y. Cheng and O. Zhou, *C. R. Phys.* **4**, 1021 (2003).

⁷C. J. Edgcombe and U. Valdré, *J. Microsc.* **203**, 188 (2001).

⁸K. A. Dean, T. P. Burgin, and B. R. Chalamala, *Appl. Phys. Lett.* **79**, 1873 (2001).

⁹K. A. Dean and B. R. Chalamala, *Appl. Phys. Lett.* **75**, 3017 (1999).

- ¹⁰V. V. Zhirnov, G. J. Wojak, W. B. Choi, J. J. Cuomo, and J. J. Hren, *J. Vac. Sci. Technol. A* **15**, 1733 (1997).
- ¹¹W. Yi, T. Jeong, S. Yu, J. Heo, C. Lee, J. Lee, W. Kim, J.-B. Yoo, and J. Kim, *Adv. Mater.* **14**, 1464 (2002).
- ¹²C. Y. Su, Z. Y. Juang, Y. L. Chen, K. C. Leou, and C. H. Tsai, *Diamond Relat. Mater.* **16**, 1393 (2007).
- ¹³K. Yu, Y. S. Zhang, F. Xu, Q. Li, Z. Q. Zhu, and Q. Wan, *Appl. Phys. Lett.* **88**, 153123 (2006).
- ¹⁴C. Wang, A. Garcia, D. C. Ingram, and M. E. Kordesh, *Electron. Lett.* **27**, 1459 (1991).
- ¹⁵M. W. Geis, N. N. Efremov, J. D. Woodhouse, M. D. McAleese, M. Marchywka, D. G. Socker, and J. F. Hochedez, *IEEE Electron Device Lett.* **12**, 456 (1991).
- ¹⁶P. W. May, S. Höhn, M. N. R. Ashfold, W. N. Wang, N. A. Fox, T. J. Davis, and J. W. Steeds, *J. Appl. Phys.* **84**, 1618 (1998).
- ¹⁷F. Le Normand, C. S. Cojocar, C. Fleaca, J. Q. Li, P. Vincent, G. Pirio, L. Gangloff, Y. Nedellec, and P. Legagneux, *Eur. Phys. J. Appl. Phys.* **38**, 115 (2007).
- ¹⁸N. A. Fox, W. N. Wang, T. J. Davis, J. W. Steeds, and P. W. May, *Appl. Phys. Lett.* **71**, 2337 (1997).
- ¹⁹N. A. Fox, S. Mary, T. J. Davis, W. N. Wang, P. W. May, A. Bewick, J. W. Steeds, and J. E. Butler, *Diamond Relat. Mater.* **6**, 1135 (1997).
- ²⁰K. P. Loh, J. S. Foord, R. G. Egdell, and R. B. Jackman, *Diamond Relat. Mater.* **6**, 874 (1997).
- ²¹P. W. May, J. C. Stone, M. N. R. Ashfold, K. R. Hallam, W. N. Wang, and N. A. Fox, *Diamond Relat. Mater.* **7**, 671 (1998).
- ²²K. M. O'Donnell, T. L. Martin, N. A. Fox, and D. Cherns, *Phys. Rev. B* **82**, 115303 (2010).
- ²³W. J. Zhang, Y. Wu, W. K. Wong, X. M. Meng, C. Y. Chan, I. Bello, Y. Lifshitz, and S. T. Lee, *Appl. Phys. Lett.* **83**, 3365 (2003).
- ²⁴N. Shankar, N. G. Glumac, M.-F. Yu, and S. P. Vanka, *Diamond Relat. Mater.* **17**, 79 (2008).
- ²⁵M. L. Terranova, S. Orlanducci, A. Fiori, E. Tamburri, V. Sessa, M. Rossi, and A. S. Barnard, *Chem. Mater.* **17**, 3214 (2005).
- ²⁶S. Orlanducci, E. Tamburri, M. L. Terranova, and M. Rossi, *Chem. Vap. Deposition* **14**, 241 (2008).
- ²⁷J. M. Rosolen, S. Tronto, M. S. Marchesin, E. C. Almeida, N. G. Ferreira, C. H. P. Poá, and S. R. P. Silva, *Appl. Phys. Lett.* **88**, 083116 (2006).
- ²⁸A. Vul, *Adv. Sci. Lett.* **3**, 110 (2010).
- ²⁹V. Guglielmotti, S. Chieppa, S. Orlanducci, E. Tamburri, F. Toschi, M. L. Terranova, and M. Rossi, *Appl. Phys. Lett.* **95**, 222113 (2009).
- ³⁰P. W. May, *Philos. Trans. R. Soc. London A* **358**, 473 (2000).
- ³¹O. A. Williams, *Diamond Relat. Mater.* **20**, 621 (2011).
- ³²O. J. L. Fox, J. O. P. Holloway, G. M. Fuge, P. W. May, and M. N. R. Ashfold, *Mater. Res. Soc. Symp. Proc.* **1203**, J17 (2009).
- ³³J. Filik, *Spectroscopy Europe* **17**, 10 (2005).
- ³⁴J. Wagner, C. Wild, and P. Koidl, *Appl. Phys. Lett.* **59**, 779 (1991).